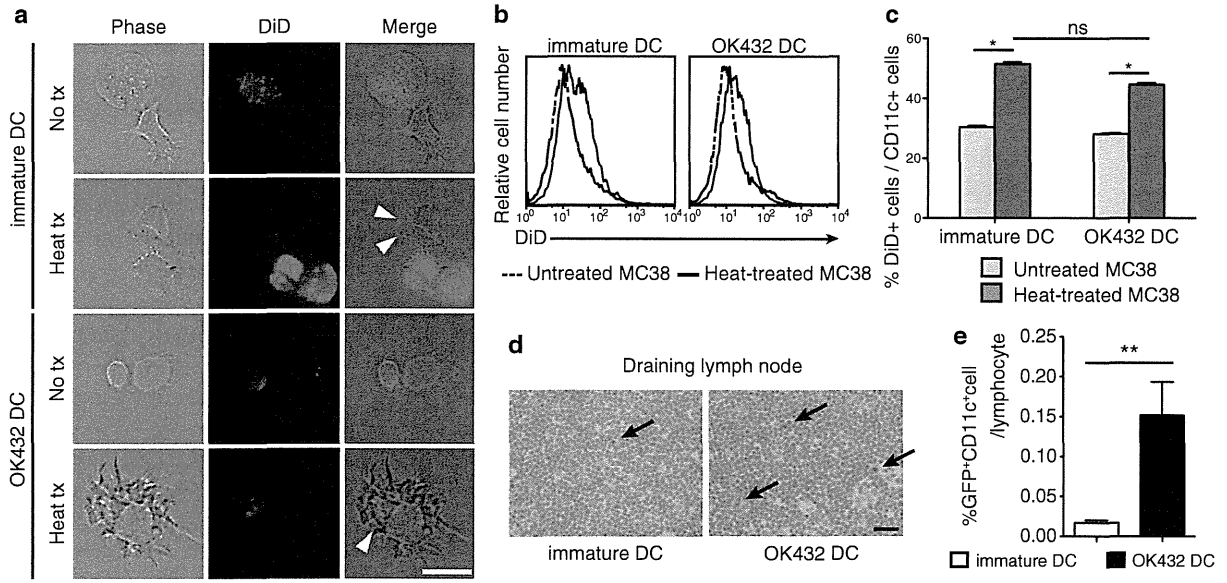

Fig. 1 Effects of OK-432 on murine bone marrow-derived DCs. **a** OK-432-stimulated DCs or immature DCs were co-incubated for 3 h with MC38 cells untreated or treated at 80 °C for 90 s after staining with DiD dye. After incubation, DC and MC38 cells were observed using a fluorescence microscope. *Arrowheads* indicate MC38 derivatives being phagocytosed by DCs. No tx, untreated MC38 cells; heat tx, heat-treated MC38 cells; *bar*, 20 μm. **b**, **c** Co-incubated MC38 cells and DCs were stained with anti-CD11c antibodies and analyzed using flow cytometry. The *histograms* show the DiD fluorescent intensity of the CD11c-positive fractions. The percentages of DiD^+ $CD11c^+$ cells in the $CD11c^+$ cell population are also shown in a *column graph*. The experiments were performed five times, and representative results are shown. Data are presented as the mean ± SE. $^*P < 0.05$. **d** The migration abilities of the DCs after intratumoral transfer were evaluated. The draining lymph nodes were harvested at 3 days after RFA followed by the DC transfer. Frozen sections were prepared and stained with anti-GFP antibodies. *Arrows* indicate the GFP-positive cells in the lymph nodes. *Bar* 20 μm. **e** The draining lymph nodes were also analyzed using flow cytometry after staining with anti-CD11c antibodies. Data were obtained from six mice in each group. Percentages of GFP^+ $CD11c^+$ cell are presented as the mean ± SE. $^{**}P < 0.01$

at 24 h after RFA treatment, and the subcutaneous tumors and the lymph nodes were harvested at 3 days after RFA. According to the immunohistochemical study involving the detection of GFP, the inguinal lymph node on the RFA-treated flank was thought to be the draining lymph node (Supplementary Fig. 3). Additionally, the number of transferred DCs in the draining lymph nodes was significantly higher in the mice treated with the OK-432-stimulated DCs than in those treated with the immature DCs (Fig. 1d, e). Our experimental results attested to the fact that the OK-432-stimulated DCs had both sufficient phagocytic ability and higher migration efficacy.

Effect of RFA in combination with the injection of OK-432-stimulated DCs on tumor growth

OK-432-stimulated DCs were used in combination therapy with RFA in this murine model (Fig. 2a). Namely, BMDCs stimulated with OK-432 were injected into RFA-treated tumor at 24 h after RFA treatment. We compared four groups of tumor-bearing mice as follows: (1) no treatment; (2) RFA only; (3) RFA with the injection of immature DCs; and (4) RFA with the injection of OK-432-stimulated DCs. Tumor volumes were measured for 10 days after treatment/no treatment. On the day after RFA, the treated tumors were covered with scars, started to shrink and had disappeared macroscopically at 4 days after RFA in all of the groups. This indicated that RFA treatment was highly effective for focal lesions. The injected DCs were detected in the treated tumors (Supplementary Fig. 3). With regard to the untreated tumors, as we previously reported, the group treated with RFA only showed an antitumor effect against distant tumors. The injection of immature DCs combined with RFA did not show any additional enhancement of the antitumor effect. On the other hand, the volumes of the untreated tumors in the group that underwent RFA combined with the injection of OK-432-stimulated DCs were strongly suppressed ($P < 0.001$) relative to other groups (Fig. 2b).

Recruitment of antigen-specific lymphocyte fractions in both splenocytes and tumor by injected OK-432-stimulated DCs

Ten days after RFA, the tumors and the spleens were harvested and analyzed using immunohistochemical staining.

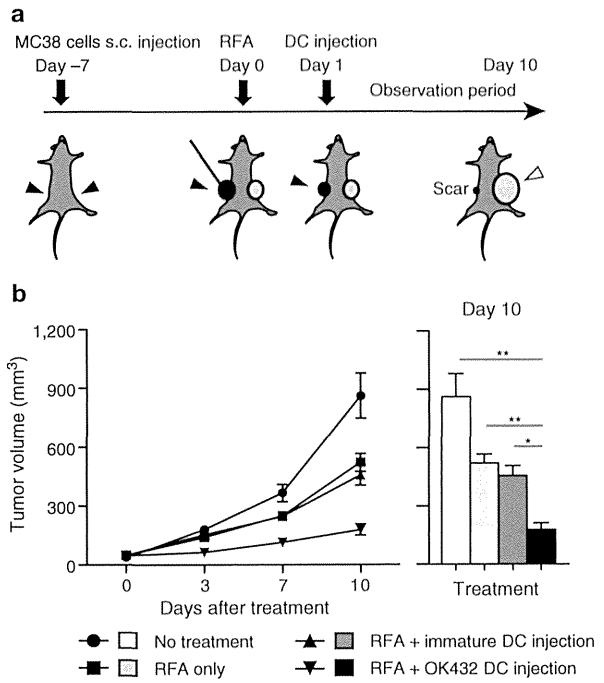

Fig. 2 Impact of injection of OK-432-stimulated DCs into murine MC38 subcutaneous tumors. **a** RFA was administered to a tumor on one flank followed by injection of 1×10^7 DCs into the treated tumor. The untreated tumor on the opposite flank was observed for 10 days. The *solid arrowheads* indicate the treatment intervention sites, and the *open arrowhead* indicates the observed untreated tumor. **b** The tumor volumes were compared among the four groups as follows: (1) no treatment; (2) RFA only; (3) RFA in combination with immature DC injection; and (4) RFA in combination with OK-432-stimulated DC injection. $n = 8$ mice per group. The data are presented as the mean ± SE. $^*P < 0.05$; $^{**}P < 0.001$

We examined the number of tumor-infiltrating CD4-positive or CD8-positive cells in the tumors by means of immunohistochemistry. The infiltration of these cells into the untreated tumors was found to be promoted by RFA. The injection of OK-432-stimulated DCs after RFA induced the additional recruitment of CD8-positive cells into the untreated tumors (Fig. 3a, b). CD11c-, CD11b- and NK1.1-positive cells were very marginal and showed no differences in number among the four groups (data not shown).

Systemically, in terms of analyzing splenocytes with flow cytometry, the number of CD4-positive and CD8-positive cells increased in the group treated with RFA in combination with OK-432-stimulated DCs. On the other hand, the CD11c and NK1.1 fractions, which were considered as DCs and NK cells, respectively, presented no difference among the four groups (Fig. 3c). In addition, we examined the effect of the injection of OK-432-stimulated DCs after RFA on inhibitory blood cells such as regulatory T cells (Tregs) and myeloid-derived suppressor cells (MDSCs) (Fig. 3c). Among CD4-positive cells, significantly fewer Tregs were detected in the group treated with RFA in combination with OK-432-stimulated DCs than in the group treated with RFA in combination with immature DCs. In the analysis of MDSCs, their rates of occurrence were not affected by treatment with either RFA alone or RFA in combination with DCs. Taking these results together, we concluded that treatment with RFA combined with OK-432-stimulated DCs enhanced the number of CD4- or CD8-positive T cells and reduced the Treg/CD4 ratio, but did not influence MDSC numbers.

Furthermore, we examined the number of tumor-specific IFN-γ-producing cells at 10 days after RFA using the ELISPOT assay. The number of IFN-γ-producing cells among splenocytes and TILs showed the same trend as the level of tumor growth control among the four groups (Fig. 3d); the group treated with RFA in combination with injected OK-432 DCs showed the most abundant specific spots. These results suggested that the augmented antitumor effects of RFA combined with OK-432-stimulated DCs depended in large part on tumor-specific immune responses by CD4 cells or CD8 cells.

Evaluation of tumor-specific immune responses in the draining lymph node after OK-432-stimulated DC transfer

CD4 T cells and CD8 T cells are now thought to have an important antitumor effect as a result of the OK-432-stimulated DC transfer. To elucidate the priming of the antigen-specific immune response, we analyzed the draining lymph nodes at 3 days after RFA focusing on CD4-positive or CD8-positive cells. CD69, the early activation marker, on CD4-positive and CD8-positive cells was examined and compared between the immature DC transfer group and the OK-432-stimulated DC transfer group. It was found that CD69 expression on both CD4-positive and CD8-positive cells was elevated in the OK-432-stimulated DC transfer group (Fig. 4a, b). The activations were also demonstrated to be tumor-specific using the IFN-γ ELISPOT assay in which each of CD4-negative and CD8-negative fractions was applied to the assay and both showed tumor-specific IFN-γ secretions (Fig. 4c).

Evaluation of the relationship between CD4-positive and CD8-positive cells and the antitumor effects of RFA and OK-432-stimulated DC transfer

We have demonstrated that combination therapy involving RFA and OK-432-stimulated DC transfer might generate enhanced antitumor effects via tumor-specific CD4-positive and CD8-positive cells. To obtain further evidence, we carried out in vivo CD4 or CD8 depletion studies in mice. Initially, we confirmed CD4 or CD8 depletion in the control in vivo study (Supplementary Fig. 4). The

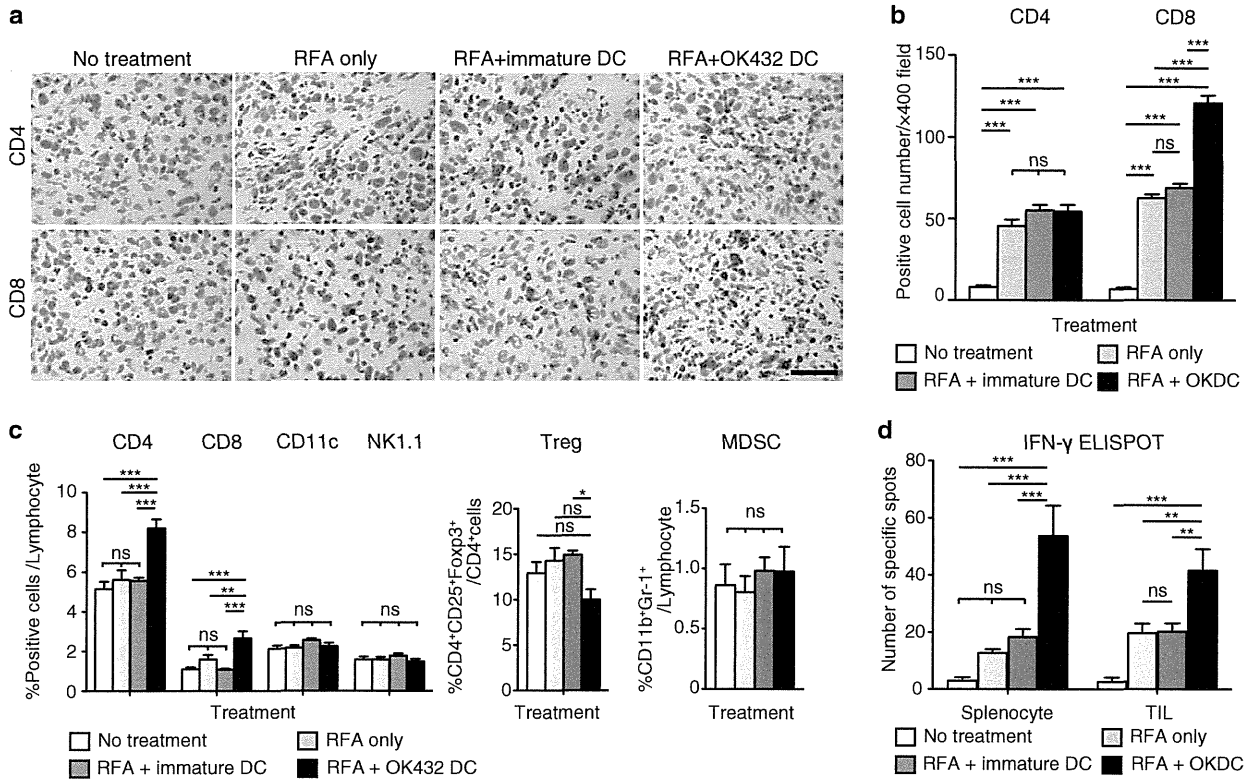

Fig. 3 Analysis of the tumor-infiltrating lymphocytes and the splenocytes after combination therapy with RFA and DC injection. **a** CD4-positive and CD8-positive cells in the observed untreated tumors were detected using immunohistochemistry at 10 days after RFA. The *black bar* represents 50 μm. **b** The number of positive cells was counted using a microscope. This was achieved by counting the number of cells in six randomly chosen tumor areas at 400-fold magnification. Three mice were used in each group. The data are presented as the mean ± SE. *** $P < 0.001$; *ns* not significant. **c** Ten days after RFA, splenocytes were stained with anti-CD4, anti-CD8, anti-NK1.1 and anti-CD11c antibodies and analyzed using flow cytometry. Regulatory T cells (Tregs) defined as $CD4^+CD25^+Foxp3^+$ cells and myeloid-derived suppressor cells (MDSCs) defined as $CD11b^+Gr\text{-}1^+$ cells were counted and compared among the four groups. Six mice were analyzed in each group. The data are presented as the mean ± SE. *$P < 0.05$; **$P < 0.01$; ***$P < 0.001$; *ns* not significant. **d** Immune responses by the splenocytes and the tumor-infiltrating lymphocytes (TILs) were examined by means of the IFN-γ enzyme-linked immunospot (ELISPOT) assay using MC38 lysate. In the assay for TILs, 1×10^5 TILs were mixed with 2×10^5 splenocytes from B6 mice and applied to the well. Six mice were analyzed in each group. The data are presented as the mean ± SE. **$P < 0.01$; ***$P < 0.001$; *ns* not significant

CD4-positive and CD8-positive fractions in the peripheral blood were greatly depleted at 7 days after injection of the antibodies. The experimental schedule was determined as follows. The depletion antibodies were injected at 1 day before and 3 days after RFA, and the tumors that were not treated with RFA were observed for 10 days. In addition, the draining lymph nodes were harvested at 3 days after RFA and analyzed (Supplementary Fig. 5). The antitumor effects of RFA treatment and the augmented effects from OK-432-stimulated DCs were cancelled out by depletion of both CD4 and CD8 cells (Fig. 5a). In the CD4 depletion study, there was no priming of the antitumor effect in the draining lymph nodes (Fig. 5b; Supplementary Fig. 6). On the other hand, in the CD8 depletion study CD4 cells were activated with tumor specificities in the draining lymph node in both groups, and the activation was stronger in the OK-432-stimulated DC transfer group (Fig. 5b; Supplementary Fig. 6). Tumor-specific reactions were also demonstrated in the splenocytes and the TILs at 10 days after RFA. There was a tendency for OK-432 DC transfer treatment to result in the recruitment of increased numbers of tumor-specific lymphocytes into the tumor on the opposite flank ($P = 0.184$; Fig. 5c). These results indicated that the tumor-specific activation of CD8 cells was necessary for the antitumor effect and was completely dependent on help from the CD4 cells.

Discussion

In the past decade, cytotoxic agents and molecular-targeted therapies have been developed, and the treatment outcomes

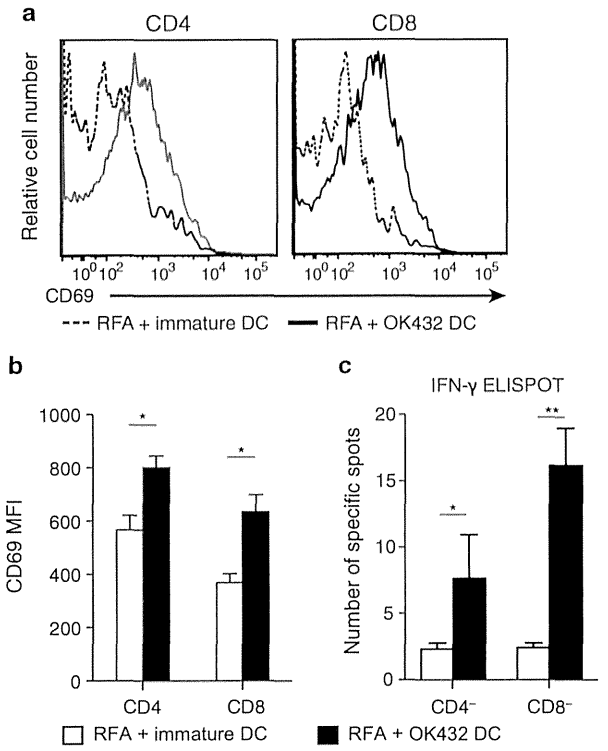

Fig. 4 Antigen-specific activation of both CD4-positive and CD8-positive cells in the draining lymph node. **a** Three days after RFA followed by DC transfer, the draining lymph node was harvested and analyzed by staining with anti-CD4 antibodies, anti-CD8 antibodies and anti-CD69 antibodies. The fluorescence intensities of CD69 in the CD4-positive and CD8-positive fractions are compared between the OK-432-stimulated DC transfer group and the immature DC transfer group. The data were obtained from six mice in each group. The *histograms* show the representative data. **b** The mean fluorescent intensities are also presented as the mean ± SE. $*P < 0.05$. **c** The antigen specificities of the T-cell activations were confirmed by means of the IFN-γ ELISPOT assay using MC38 lysate. After CD4 or CD8 depletion using CD4 and CD8 magnetic beads, the lymphocytes from the draining lymph nodes were submitted to IFN-γ ELISPOT assay. Data were obtained from six mice in each group. $*P < 0.05$; $**P < 0.01$

for various cancers have improved. However, few patients with advanced cancers have been completely cured, and thus, new strategies for anticancer therapy are required. Immunotherapy is considered to have the potential to effectively treat such advanced cancers, and many different approaches have been explored. For the utilization of the adoptive immune response in a cancer therapy, DCs are a key constituent of the immune system. This is because of their natural potential to present tumor-associated antigens to $CD4^+$ and $CD8^+$ lymphocytes and also to control both immune tolerance and immunity [21]. Thus, DCs are considered as an important target for cancer immunotherapy. Many trials and studies have been carried out regarding immunotherapy for cancer using DCs, some of which have been reported to have pronounced effects [22–25]. In recent studies, it has been revealed that RFA treatment induces tumor-specific T-cell responses, which is known as the abscopal effect; this has been mainly reported in radiotherapy studies and is augmented with combined immunotherapies [26, 27]. Brok et al. [28] have previously reported on the vaccination effects of combination therapy involving RFA and CTLA-4 antibody.

To our knowledge, this is the first study that has demonstrated using a murine metastatic cancer model that RFA in combination with focal DC injection could enhance the antitumor effects of RFA alone. Our results showed that immature DCs made no additional immunological contribution to RFA. In the analysis of draining lymph nodes, few transferred DCs were detected after the injection of immature DCs. It appeared that immature DCs did not act as sentinels in the adoptive immune system, partially because they exhibited low expression of CCR7 (the main molecule that promotes DC migration [29]), even though elevation of CCR7 expression using OK-432 was very modest in our study. There is another possibility immature DCs are easily lysed and excluded by the host immune system [30]. On the other hand, mature DCs can escape cell lysis [31].

Utilization of OK-432-stimulated DCs improved the number of migrating transferred DCs in the present study. These DCs, which could act as sentinels for immunity, induced expansion in the number of tumor-specific lymphocytes in the draining lymph nodes, in the splenocytes and in the distant nontreated tumors, without systemic expansion of inhibitory cells such as Tregs or MDSCs. We also demonstrated that these augmented antitumor effects after OK-432-stimulated DC transfer were primed in the draining lymph nodes with tumor-specific activations of CD4-positive and CD8-positive cells; it was proved that without CD4-positive or CD8-positive cells, both the antitumor effect by RFA and the additional effect of the injection of OK-432-stimulated DCs disappeared completely. In addition, the in vivo CD4 depletion study revealed that tumor-specific activations of CD8-positive cells were not seen in the draining lymph nodes in both groups after the injection of immature DCs and OK-432-stimulated DC injection; in other words, tumor-specific CD8 activation depended on CD4-positive cells entirely. In the CD8 depletion study, on the other hand, we found that tumor-specific CD4-positive cells appeared in the draining lymph nodes, the splenocyte population and the untreated tumor on the opposite flank, and these lymphocytes were considered to be CD4-positive cells. In the tumor-infiltrating lymphocytes, there was a tendency for more tumor-specific CD4-positive cells to be recruited after treatment involving OK-432-stimulated DC transfer. Many researchers have demonstrated the contribution of CD4 cells to cytotoxicity

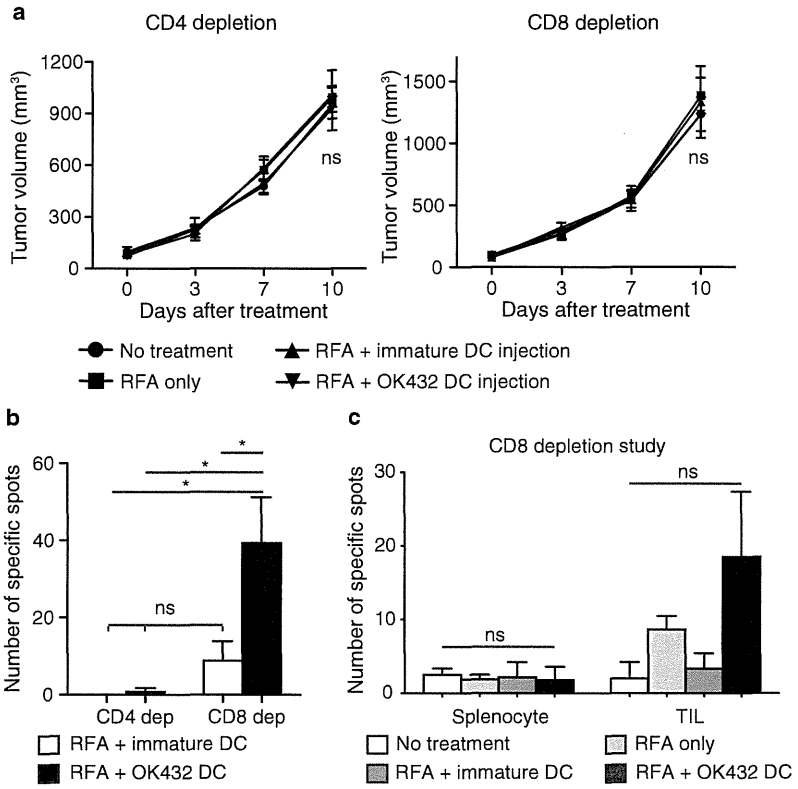

Fig. 5 The augmented antitumor effects depended on both CD4-positive and CD8-positive cells. **a** For in vivo CD4 or CD8 depletion, monoclonal antibodies specific to CD4 (GK1.5) or CD8 (2.43), respectively, were injected intraperitoneally at 1 day before and 3 days after RFA. Tumor volumes were compared among the four groups for 10 days after RFA. In each experiment, data were obtained from four mice per group and are presented as the mean ± SE. *ns* not significant. **b** The draining lymph nodes were harvested at 3 days after RFA and analyzed for their tumor specificities using the IFN-γ ELISPOT assay. Two mice were used in each group. Data are shown as the mean ± SE. $*P < 0.005$; *ns* not significant. **c** In the CD8 depletion study, splenocytes and tumor-infiltrating lymphocytes (TILs) were evaluated for their tumor specificities using the IFN-γ ELISPOT assay as described in Fig. 3. Four mice were used in each group. Data are shown as the mean ± SE. *ns* not significant

[32, 33]. However, in our experimental models, tumor-specific CD4-positive cells were not observed to contribute to the antitumor effect. Summarizing the above, in our study, the CD4-positive cells were required for the priming of the immune responses, and the CD8-positive cells acted as the effector cells after help from the CD4-positive cells.

In conclusion, we consider on the basis of our preclinical findings regarding combination therapy involving OK-432-stimulated DCs with RFA for the treatment of metastatic liver cancer that clinical trials can now proceed. It is anticipated that this combination therapy will be markedly superior to RFA single therapy.

Acknowledgments The authors thank Ms. Fushimi and Ms. Baba for technical support. This study was supported by research grants from the Ministry of Education, Culture, Sports, Science and Technology of Japan.

Conflict of interest The authors received financial support for this study from Chugai Pharmaceutical Co., Ltd.

References

1. Ruiterkamp J, Ernst MF, de Munck L, van der Heiden, van der Loo M, Bastiaannet E, van de Poll-Franse LV, Bosscha K, Tjan-Heijnen VC, Voogd AC (2011) Improved survival of patients with primary distant metastatic breast cancer in the period of 1995–2008. A nationwide population-based study in the Netherlands. Breast Cancer Res Treat 128(2):495–503. doi:10.1007/s10549-011-1349-x
2. Simmonds PC, Primrose JN, Colquitt JL, Garden OJ, Poston GJ, Rees M (2006) Surgical resection of hepatic metastases from colorectal cancer: a systematic review of published studies. Br J Cancer 94(7):982–999. doi:10.1038/sj.bjc.6603033
3. Nordlinger B, Guiguet M, Vaillant JC, Balladur P, Boudjema K, Bachellier P, Jaeck D (1996) Surgical resection of colorectal carcinoma metastases to the liver. A prognostic scoring system to improve case selection, based on 1568 patients. Association Francaise de Chirurgie. Cancer 77(7):1254–1262
4. Bentrem DJ, Dematteo RP, Blumgart LH (2005) Surgical therapy for metastatic disease to the liver. Annu Rev Med 56:139–156. doi:10.1146/annurev.med.56.082103.104630
5. Meyers MO, Sasson AR, Sigurdson ER (2003) Locoregional strategies for colorectal hepatic metastases. Clin Colorectal Cancer 3(1):34–44. doi:10.3816/CCC.2003.n.010

6. Napoletano C, Taurino F, Biffoni M, De Majo A, Coscarella G, Bellati F, Rahimi H, Pauselli S, Pellicciotta I, Burchell JM, Gaspari LA, Ercoli L, Rossi P, Rughetti A (2008) RFA strongly modulates the immune system and anti-tumor immune responses in metastatic liver patients. Int J Oncol 32(2):481–490
7. Nobuoka D, Motomura Y, Shirakawa H, Yoshikawa T, Kuronuma T, Takahashi M, Nakachi K, Ishii H, Furuse J, Gotohda N, Takahashi S, Nakagohri T, Konishi M, Kinoshita T, Komori H, Baba H, Fujiwara T, Nakatsura T (2012) Radiofrequency ablation for hepatocellular carcinoma induces glypican-3 peptide-specific cytotoxic T lymphocytes. Int J Oncol 40(1):63–70. doi:10.3892/ijo.2011.1202
8. Iida N, Nakamoto Y, Baba T, Nakagawa H, Mizukoshi E, Naito M, Mukaida N, Kaneko S (2010) Antitumor effect after radiofrequency ablation of murine hepatoma is augmented by an active variant of CC Chemokine ligand 3/macrophage inflammatory protein-1 alpha. Cancer Res 70(16):6556–6565. doi:10.1158/0008-5472.CAN-10-0096
9. Banchereau J, Briere F, Caux C, Davoust J, Lebecque S, Liu YJ, Pulendran B, Palucka K (2000) Immunobiology of dendritic cells. Annu Rev Immunol 18:767–811. doi:10.1146/annurev.immunol.18.1.767
10. Nakamoto Y, Mizukoshi E, Tsuji H, Sakai Y, Kitahara M, Arai K, Yamashita T, Yokoyama K, Mukaida N, Matsushima K, Matsui O, Kaneko S (2007) Combined therapy of transcatheter hepatic arterial embolization with intratumoral dendritic cell infusion for hepatocellular carcinoma: clinical safety. Clin Exp Immunol 147(2):296–305. doi:10.1111/j.1365-2249.2006.03290.x
11. Ryoma Y, Moriya Y, Okamoto M, Kanaya I, Saito M, Sato M (2004) Biological effect of OK-432 (picibanil) and possible application to dendritic cell therapy. Anticancer Res 24(5C):3295–3301
12. Nakahara S, Tsunoda T, Baba T, Asabe S, Tahara H (2003) Dendritic cells stimulated with a bacterial product, OK-432, efficiently induce cytotoxic T lymphocytes specific to tumor rejection peptide. Cancer Res 63(14):4112–4118
13. Okamoto M, Oshikawa T, Tano T, Ahmed SU, Kan S, Sasai A, Akashi S, Miyake K, Moriya Y, Ryoma Y, Saito M, Sato M (2006) Mechanism of anticancer host response induced by OK-432, a streptococcal preparation, mediated by phagocytosis and Toll-like receptor 4 signaling. J Immuno ther 29(1):78–86
14. Hovden AO, Karlsen M, Jonsson R, Appel S (2012) The bacterial preparation OK432 induces IL-12p70 secretion in human dendritic cells in a TLR3 dependent manner. PLoS ONE 7(2):e31217. doi:10.1371/journal.pone.0031217
15. Nakamoto Y, Mizukoshi E, Kitahara M, Arihara F, Sakai Y, Kakinoki K, Fujita Y, Marukawa Y, Arai K, Yamashita T, Mukaida N, Matsushima K, Matsui O, Kaneko S (2011) Prolonged recurrence-free survival following OK432-stimulated dendritic cell transfer into hepatocellular carcinoma during transarterial embolization. Clin Exp Immunol 163(2):165–177. doi:10.1111/j.1365-2249.2010.04246.x
16. Inaba K, Inaba M, Romani N, Aya H, Deguchi M, Ikehara S, Muramatsu S, Steinman RM (1992) Generation of large numbers of dendritic cells from mouse bone marrow cultures supplemented with granulocyte/macrophage colony-stimulating factor. J Exp Med 176(6):1693–1702
17. Mizukoshi E, Nakamoto Y, Marukawa Y, Arai K, Yamashita T, Tsuji H, Kuzushima K, Takiguchi M, Kaneko S (2006) Cytotoxic T cell responses to human telomerase reverse transcriptase in patients with hepatocellular carcinoma. Hepatology 43(6):1284–1294. doi:10.1002/hep.21203
18. Nakamoto Y, Suda T, Momoi T, Kaneko S (2004) Different procarcinogenic potentials of lymphocyte subsets in a transgenic mouse model of chronic hepatitis B. Cancer Res 64(9):3326–3333
19. Okamoto M, Furuichi S, Nishioka Y, Oshikawa T, Tano T, Ahmed SU, Takeda K, Akira S, Ryoma Y, Moriya Y, Saito M, Sone S, Sato M (2004) Expression of toll-like receptor 4 on dendritic cells is significant for anticancer effect of dendritic cell-based immunotherapy in combination with an active component of OK-432, a streptococcal preparation. Cancer Res 64(15):5461–5470. doi:10.1158/0008-5472.CAN-03-4005
20. Hill KS, Errington F, Steele LP, Merrick A, Morgan R, Selby PJ, Georgopoulos NT, O'Donnell DM, Melcher AA (2008) OK432-activated human dendritic cells kill tumor cells via CD40/CD40 ligand interactions. J Immunol 181(5):3108–3115
21. Banchereau J, Steinman RM (1998) Dendritic cells and the control of immunity. Nature 392(6673):245–252. doi:10.1038/32588
22. Timmerman JM, Czerwinski DK, Davis TA, Hsu FJ, Benike C, Hao ZM, Taidi B, Rajapaksa R, Caspar CB, Okada CY, van Beckhoven A, Liles TM, Engleman EG, Levy R (2002) Idiotype-pulsed dendritic cell vaccination for B-cell lymphoma: clinical and immune responses in 35 patients. Blood 99(5):1517–1526
23. Banchereau J, Palucka AK, Dhodapkar M, Burkeholder S, Taquet N, Rolland A, Taquet S, Coquery S, Wittkowski KM, Bhardwaj N, Pineiro L, Steinman R, Fay J (2001) Immune and clinical responses in patients with metastatic melanoma to CD34(+) progenitor-derived dendritic cell vaccine. Cancer Res 61(17):6451–6458
24. Okada H, Kalinski P, Ueda R, Hoji A, Kohanbash G, Donegan TE, Mintz AH, Engh JA, Bartlett DL, Brown CK, Zeh H, Holtzman MP, Reinhart TA, Whiteside TL, Butterfield LH, Hamilton RL, Potter DM, Pollack IF, Salazar AM, Lieberman FS (2011) Induction of CD8 + T-cell responses against novel glioma-associated antigen peptides and clinical activity by vaccinations with {alpha}-type 1 polarized dendritic cells and polyinosinic-polycytidylic acid stabilized by lysine and carboxymethylcellulose in patients with recurrent malignant glioma. J Clin Oncol 29(3):330–336. doi:10.1200/JCO.2010.30.7744
25. Suso EM, Dueland S, Rasmussen AM, Vetrhus T, Aamdal S, Kvalheim G, Gaudernack G (2011) hTERT mRNA dendritic cell vaccination: complete response in a pancreatic cancer patient associated with response against several hTERT epitopes. Cancer Immunol Immunother 60(6):809–818. doi:10.1007/s00262-011-0991-9
26. Frey B, Weiss EM, Rubner Y, Wunderlich R, Ott OJ, Sauer R, Fietkau R, Gaipl US (2012) Old and new facts about hyperthermia-induced modulations of the immune system. Int J Hyperthermia 28(6):528–542. doi:10.3109/02656736.2012.677933
27. Rubner Y, Wunderlich R, Ruhle PF, Kulzer L, Werthmoller N, Frey B, Weiss EM, Keilholz L, Fietkau R, Gaipl US (2012) How does ionizing irradiation contribute to the induction of anti-tumor immunity? Front Oncol 2:75. doi:10.3389/fonc.2012.00075
28. den Brok MH, Sutmuller RP, van der Voort R, Bennink EJ, Figdor CG, Ruers TJ, Adema GJ (2004) In situ tumor ablation creates an antigen source for the generation of antitumor immunity. Cancer Res 64(11):4024–4029. doi:10.1158/0008-5472.CAN-03-3949
29. Forster R, Schubel A, Breitfeld D, Kremmer E, Renner-Muller I, Wolf E, Lipp M (1999) CCR7 coordinates the primary immune response by establishing functional microenvironments in secondary lymphoid organs. Cell 99(1):23–33
30. Ferlazzo G, Tsang ML, Moretta L, Melioli G, Steinman RM, Munz C (2002) Human dendritic cells activate resting natural killer (NK) cells and are recognized via the NKp30 receptor by activated NK cells. J Exp Med 195(3):343–351
31. Morandi B, Mortara L, Chiossone L, Accolla RS, Mingari MC, Moretta L, Moretta A, Ferlazzo G (2012) Dendritic cell editing by activated natural killer cells results in a more protective cancer-specific immune response. PLoS ONE 7(6):e39170. doi:10.1371/journal.pone.0039170

32. Ab BK, Kiessling R, Van Embden JD, Thole JE, Kumararatne DS, Pisa P, Wondimu A, Ottenhoff TH (1990) Induction of antigen-specific CD4+ HLA-DR-restricted cytotoxic T lymphocytes as well as nonspecific nonrestricted killer cells by the recombinant mycobacterial 65-kDa heat-shock protein. Eur J Immunol 20(2):369–377. doi:10.1002/eji.1830200221

33. Bourgault I, Gomez A, Gomard E, Picard F, Levy JP (1989) A virus-specific CD4+ cell-mediated cytolytic activity revealed by CD8+ cell elimination regularly develops in uncloned human antiviral cell lines. J Immunol 142(1):252–256

HEPATOLOGY
Official Journal of the American Association for the Study of Liver Diseases

Hepatic Interferon-Stimulated Genes Are Differentially Regulated in the Liver of Chronic Hepatitis C Patients With Different Interleukin-28B Genotypes

Masao Honda,[1,2] Takayoshi Shirasaki,[2] Tetsuro Shimakami,[1] Akito Sakai,[1] Rika Horii,[1] Kuniaki Arai,[1] Tatsuya Yamashita,[1] Yoshio Sakai,[1] Taro Yamashita,[1] Hikari Okada,[1] Kazuhisa Murai,[1] Mikiko Nakamura,[2] Eishiro Mizukoshi,[1] and Shuichi Kaneko[1]

Pretreatment up-regulation of hepatic interferon (IFN)-stimulated genes (ISGs) has a stronger association with the treatment-resistant interleukin (IL)28B minor genotype (MI; TG/GG at rs8099917) than with the treatment-sensitive IL28B major genotype (MA; TT at rs8099917). We compared the expression of ISGs in the liver and blood of 146 patients with chronic hepatitis C who received pegylated IFN and ribavirin combination therapy. Gene expression profiles in the liver and blood of 85 patients were analyzed using an Affymetrix GeneChip (Affymetrix, Santa Clara, CA). ISG expression was correlated between the liver and blood of the MA patients, whereas no correlation was observed in the MI patients. This loss of correlation was the result of the impaired infiltration of immune cells into the liver lobules of MI patients, as demonstrated by regional gene expression analysis in liver lobules and portal areas using laser capture microdissection and immunohistochemical staining. Despite having lower levels of immune cells, hepatic ISGs were up-regulated in the liver of MI patients and they were found to be regulated by multiple factors, namely, IL28A/B, IFN-λ4, and wingless-related MMTV integration site 5A (WNT5A). Interestingly, WNT5A induced the expression of ISGs, but also increased hepatitis C virus replication by inducing the expression of the stress granule protein, GTPase-activating protein (SH3 domain)-binding protein 1 (G3BP1), in the Huh-7 cell line. In the liver, the expression of WNT5A and its receptor, frizzled family receptor 5, was significantly correlated with G3BP1. *Conclusions:* Immune cells were lost and induced the expression of other inflammatory mediators, such as WNT5A, in the liver of IL28B minor genotype patients. This might be related to the high level of hepatic ISG expression in these patients and the treatment-resistant phenotype of the IL28B minor genotype. (HEPATOLOGY 2014;59:828-838)

Interferon (IFN) and ribavirin (RBV) combination therapy has been a popular modality for treating patients with chronic hepatitis C (CHC); however, ~50% of patients usually relapse, particularly those with hepatitis C virus (HCV) genotype 1b and a high viral load.[1] The recently developed direct-acting antiviral drug, telaprevir, combined with pegylated (Peg)-IFN plus RBV, significantly improved sustained virologic response (SVR) rates; however, the SVR rate was not satisfactory (29%-33%) in patients who had no

Abbreviations: ALT, alanine aminotransferase; AST, aspartate aminotransferase; CCL, CC chemokine ligand; CHC, chronic hepatitis C; CLLs, cells in liver lobules; CPAs, cells in portal areas; CXCL10/IP-10, chemokine (C-X-C motif) ligand 10/interferon-gamma-induced protein 10; CXCR3, chemokine (C-X-C motif) receptor 3; DCs, dendritic cells; DVL, disheveled; FZD5, frizzled family receptor 5; G3BP1, GTPase-activating protein (SH3 domain)-binding protein 1; GGT, gamma-glutamyl transpeptidase; HCV, hepatitis C virus; IFI44, interferon-induced protein 44; IFIT1, interferon-induced protein with tetratricopeptide repeats 1; IFN, interferon; IHC, immunohistochemical; IL, interleukin; ISGs, interferon-stimulated genes; JFH-1, Japanese fulminant hepatitis type 1; LCM, laser capture microdissection; MA, major genotype; MAd, major genotype, down-regulated; MAu, major genotype, up-regulated; MI, minor genotype; Mx, myxovirus (influenza virus) resistance; NK, natural killer; OAS2, 2′-5′-oligoadenylate synthetase 2; PALT, portal-tract-associated lymphoid tissue; Peg_IFN, pegylated IFN; RBV, ribavirin; RTD-PCR, real-time detection polymerase chain reaction; SG, stress granule; siRNA, small interfering RNA; SVR, sustained virologic response; WNT5A, wingless-related MMTV integration site 5A.

From the [1]Department of Gastroenterology, Kanazawa University Graduate School of Medicine, Kanazawa, Japan; and [2]Department of Advanced Medical Technology, Kanazawa University Graduate School of Health Medicine, Kanazawa, Japan.

Received May 31, 2013; accepted September 30, 2013.

response to previous therapy.[2] Therefore, IFN responsiveness is still an essential clinical determinant for treatment response to triple (Peg-IFN+RBV+DAA) therapy.

A recent landmark genome-wide association study identified a polymorphism in the interleukin (IL)28B, IFN-λ3) gene that was associated with either a sensitive (major genotype; MA) or resistant (minor genotype; MI) treatment response to Peg-IFN and RBV combination therapy and was characterized by either up- (-u) or down-regulation (-d) of interferon-stimulated genes (ISGs).[3-5] However, the underlying mechanism for the association of this polymorphism and treatment response has not been clarified. Previously, we showed that up-regulation of the pretreatment expression of hepatic ISGs was associated with an unfavorable treatment outcome and was closely related to the treatment-resistant IL28B genotype (TG or GG at rs8099917).[6] It could be speculated that the pretreatment activation of ISGs would repress additional induction of ISGs after treatment with exogenous IFN. However, it is unknown how hepatic ISGs are up-regulated in treatment-resistant CHC patients and why patients with high levels of ISG expression cannot eliminate HCV. Therefore, other mechanisms should be involved in the unfavorable treatment outcome of patients with the treatment-resistant IL28B genotype.

In the present study, we performed gene expression profiling in the liver and blood and compared the expression of ISGs between them. Furthermore, ISG expression in liver lobules and portal areas was analyzed separately using a laser capture microdissection (LCM) method. Finally, we identified an immune factor that is up-regulated in patients with the treatment-resistant IL28B genotype and mediates favorable signaling for HCV replication.

Materials and Methods

Patients. We analyzed 168 patients with CHC who had received Peg-IFN-α2b (Schering-Plough K.K., Tokyo, Japan) and RBV combination therapy for 48 weeks at the Graduate School of Medicine, Kanazawa University Hospital, Japan and its related hospitals, as reported previously (Table 1 and Supporting Table 1).[6]

Preparation of Liver Tissue and Blood Samples. A liver biopsy was performed on samples from 168 patients, and blood samples were obtained from 146 of these patients before starting therapy (Table 1 and Supporting Table 1). Detailed procedures are described in the Supporting Materials and Methods.

Affymetrix GeneChip Analysis. Liver tissue samples from 91 patients and blood samples from 85 patients were analyzed using an Affymetrix GeneChip (Affymetrix, Santa Clara, CA). LCM analysis was performed in 5 MAu, MAd, and MI patients. Affymetrix GeneChip analysis and LCM were performed, as described previously.[6,7] Detailed procedures are described in the Supporting Materials and Methods.

Hierarchical Clustering and Pathway Analysis of GeneChip Data. GeneChip data analysis was performed using BRB-Array Tools (http://linus.nci.nih.gov/BRB-ArrayTools.htm), as described previously.[7] Pathway analysis was performed using MetaCore (Thomson Reuters, New York, NY). Detailed procedures are described in the Supporting Materials and Methods.

Quantitative Real-Time Detection Polymerase Chain Reaction, Cell Lines, Cell Migration Assay, Vector Preparation, HCV Replication Analysis, and Statistical Analysis. These procedures are described in detail in the Supplemental Material and Methods.

Results

Differential ISG Expression in Liver and Blood of Patients With Different IL28B Genotypes. Previously, we showed that pretreatment up-regulation of hepatic ISGs was associated with an unfavorable treatment outcome and was closely related to the treatment-resistant IL28B MI (TG or GG at rs8099917).[6] To examine whether expression of hepatic ISGs would reflect the expression of blood ISGs, we compared ISG expression between the liver and blood. We utilized three ISGs (interferon-induced protein 44 [IFI44], interferon-induced protein with

Address reprint requests to: Shuichi Kaneko, M.D., Ph.D., Department of Gastroenterology, Graduate School of Medicine, Kanazawa University, Takara-Machi 13-1, Kanazawa 920-8641, Japan. E-mail: skaneko@m-kanazawa.jp; fax: +81-76-234-4250.

Copyright © 2014 by the American Association for the Study of Liver Diseases.

View this article online at wileyonlinelibrary.com.
DOI 10.1002/hep.26788
Potential conflict of interest: Nothing to report.
Additional Supporting Information may be found in the online version of this article.

Table 1. Clinical Characteristics of 146 Patients Whose Liver and Blood Samples Were Analyzed by RT-PCR

	Major (MA)				Minor (MI)		
Clinical Category	Major ISG Up (MAu)		Major ISG Down (MAd)				*P* Value
No. of patients	n = 42		n = 68		n = 36		NA
Age and sex							
Age (years)	55	(30-72)	56	(31-72)	55	(30-73)	NS
Sex (M vs. F)	27 vs. 15		34 vs. 34		19 vs. 17		NS
Treatment responses							
SVR/TR/NR	24/12/6		30/33/6		6/7/23*		MAu vs. MI < 0.0001, MAd vs. MI < 0.0001
IL28B genotype (TT vs. TG+GG)	TT		TT		TG/GG (31/5)		NA
Liver factors							
F stage (1/2/3/4)	14/13/11/4		30/20/11/7		14/8/10/4		NS
A grade (A0-1 vs. A2-3)	16 vs. 26		37 vs. 31		20 vs. 16		NS
ISGs (Mx1, IFI44, IFIT1)	3.83*	(2.14-9.48)	1.30*	(0.36-2.08)	5.52*	(0.86-17.3)	MAu vs. MAd < 0.0001, MAu vs. MI < 0.0001, MAd vs. MI < 0.0001
IL28A/B	41.3*	(4-151)	11.7*	(1-53)	22.7*	(3-93)	MAu vs. MAd < 0.0001, MAu vs. MI = 0.0004, MAd vs. MI = 0.031
Blood factors							
ISGs (Mx1, IFI44, IFIT1)	11.1*	(2.78-24.9)	4.76	(0.41-20.6)	5.64	(0.71-2.8)	MAu vs. MAd < 0.0001, MAu vs. MI < 0.0001
IL28A/B	1.6	(0.1-7.7)	1.3	(0.2-6.4)	1.3	(0.3-3.6)	NS
Laboratory parameters							
HCV-RNA (KIU/mL)	2,430	(160-5,000)	2,692	(140-5,000)	1,854*	(126-5,000)	MAd vs. MI = 0.017
BMI (kg/m2)	24	(18.7-31.9)	24	(16.3-34.7)	22.8	(19.1-30.5)	NS
AST (IU/L)	86*	(22-258)	54	(18-192)	64	(21-178)	MAu vs. MAd = 0.0008
ALT (IU/L)	112*	(17-376)	75	(16-345)	79	(18-236)	MAu vs. MAd = 0.023
γ-GTP (IU/L)	99*	(21-392)	47	(4-367)	74	(20-298)	MAu vs. MAd = 0.0003
WBC (/mm3)	4,761	(2,100-8,100)	4,982	(2,800-9,100)	4,823	(2,500-8,200)	NS
Hb (g/dL)	14.1	(11.4-16.7)	14.1	(9.3-16.9)	13.9	(11.2-16.4)	NS
PLT (× 104/mm3)	15.2	(9.2-27.8)	16.8	(7-39.4)	16.3	(9-27.8)	NS
TG (mg/dL)	112	(42-248)	102	(42-260)	136*	(30-323)	MAd vs. MI = 0.02
T-Chol (mg/dL)	162	(90-221)	169	(107-229)	167	(81-237)	NS
LDL-Chol (mg/dL)	77	(36-123)	83*	(42-134)	72	(29-107)	MAd vs. MI = 0.04
HDL-Chol (mg/dL)	40	(18-67)	43	(27-71)	47*	(27-82)	NS
Viral factors							
ISDR mutations ≦ 1 vs. ≧ 2	23 vs. 19*		51 vs. 17		26 vs. 10		MAu vs. MAd = 0.02
Core aa 70 (wild-type vs. mutant)	24 vs. 18		42 vs. 22		16 vs. 20*		MAd vs. MI = 0.02

*$P < 0.05$.

Abbreviations: BMI, body mass index; ALT, alanine aminotransferase; WBC, leukocytes; Hb, hemoglobin; PLT, platelets; TG, triglycerides; T-chol, total cholesterol; LDL-chol, low density lipoprotein cholesterol; HDL-chol, high density lipoprotein cholesterol; NA, not applicable; NS, not significant.

tetratricopeptide repeats 1 [IFIT1], and myxovirus (influenza virus) resistance [Mx1]) with a high dynamic range, comparable relative expression, and good predictive performance.[6] Mean values of the three ISGs detected by real-time detection polymerase chain reaction (RTD-PCR) in 168 liver tissue samples (Supporting Table 1) showed a significant up-regulation of their expression in nonresponder or treatment-resistant IL28B MI (TG/GG; rs8099917) patients, compared to responder (SVR+TR) or treatment-sensitive IL28B MA (TT; rs8099917) patients, as reported previously (Fig. 1A and Supporting Fig. 1A).[6] However, ISG expression in 146 blood samples (Table 1) showed no difference between responders and nonresponders or the IL28B major and minor genotypes (Fig. 1B and Supporting Fig. 1B). To explore these findings further, gene expression profiling using Affymetrix GeneChips was performed on liver and blood samples from 85 patients (Supporting Tables 2 and 3), and the expression of 37 representative ISGs[6] was compared (Fig. 1C-E). MA patients were divided into two groups according to their ISG expression pattern in the liver: MAu and MAd. MI patients expressed ISGs at a higher level than MAu patients. Interestingly, ISG expression in MA patients showed a similar expression pattern in liver and blood, and ISGs were up-regulated in MAu patients and down-regulated in the MAd patients. However, MI patients showed a different ISG expression pattern in liver and blood, where ISGs were up-regulated in the liver, but down-regulated in the blood (Fig. 1C). The correlation of the mean values of the three ISGs (IFI44, IFIT1, and Mx1) between liver and blood from 146 patients demonstrated a significant correlation between values in MA patients (Fig. 1D), whereas no correlation was observed in MI patients (Fig. 1E). Interestingly, ISG expression correlated significantly between liver and blood of responders, but not of nonresponders, in MA and MI patients (Supporting Fig. 1C-F). These results indicate that the correlation of ISG expression in the liver and blood is an important predictor of treatment response.

Clinical Characteristics of IL28B MA Patients With Up- and Down-Regulated ISGs and IL28B MI Patients. From the expression pattern of ISGs and mean values of the three ISGs (IFI44, IFIT1, and Mx1), we could use receiver operating characteristic curve analysis to set a threshold of 2.1-fold to differentiate MAu and MAd patients. Following this criterion, 42 MAu, 68 MAd, and 36 MI patients (total, 146) were grouped (Table 1). Hepatic ISG expression was highest in MI patients, whereas blood ISG expression was highest in MAu patients. Conversely, hepatic IL28A/B (IFN-λ2/3) expression was highest in MAu patients, whereas blood IL28A/B expression showed no difference among the three groups. Serum alanine aminotransferase (ALT), aspartate aminotransferase (AST), and gamma-glutamyl transpeptidase (GGT) levels were significantly higher in MAu patients than in MAd patients. Interestingly, serum ALT levels were significantly correlated with ISG expression in MA patients, but not in MI patients (Supporting Fig. 2E,F).

Gene expression profiling in peripheral immune cells showed the presence of active inflammation in MAu patients, whereas the inactive or remissive phase of inflammation was observed in MAd patients. In contrast, monophasic and intermediate inflammation existed in MI patients (Supporting Fig. 3).

Reduced Number of Immune Cells in the Liver Lobules of IL28B MI Patients. To examine the discordant expression of ISGs in liver and blood of MI patients, we performed LCM to collect cells in liver lobules (CLLs) and cells in portal areas (CPAs) separately from each of five liver biopsied samples from MAu, MAd, and MI patients (Fig. 2A). Interestingly, the ISG expression pattern in CLLs from MA patients was similar to that of CPAs, and ISGs were up-regulated in MAu patients and down-regulated in MAd patients. ISG expression in CLLs from the MI patients was different to that in CPAs, and ISGs were up-regulated in CLLs, but down-regulated in CPAs (Fig. 2A). We hypothesized that the discordance of ISG expression between CLLs and CPAs in MI patients might be the result of the lower number of immune cells that infiltrated the liver lobules of these patients. To prove this hypothesis, immunohistochemical (IHC) staining was performed (Fig. 2B). IHC staining showed that IFI44 was strongly expressed in the cytoplasm and nucleus of CLLs from MI patients, whereas it was intermediately expressed in MAu patients and weakly expressed in MAd patients. Interestingly, IFI44 was strongly expressed in CPAs of MAu patients and weakly expressed in CPAs of MAd patients, showing a correlation between expression in CLLs and CPAs of MA patients, whereas ILI44 expression was relatively weak in CPAs, compared with CLLs, in MI patients (Fig. 2B). In the same section of the specimens, there were less CD163-positive monocytes and macrophages in MI patients than in MAu and MAd patients. Similarly, there were fewer CD8-positive T cells in MI patients than in MAu and MAd patients (Fig. 2B). Semiquantitative evaluation of CD163- and CD8-positive lymphocytes in liver lobules showed a significantly lower number of cells in

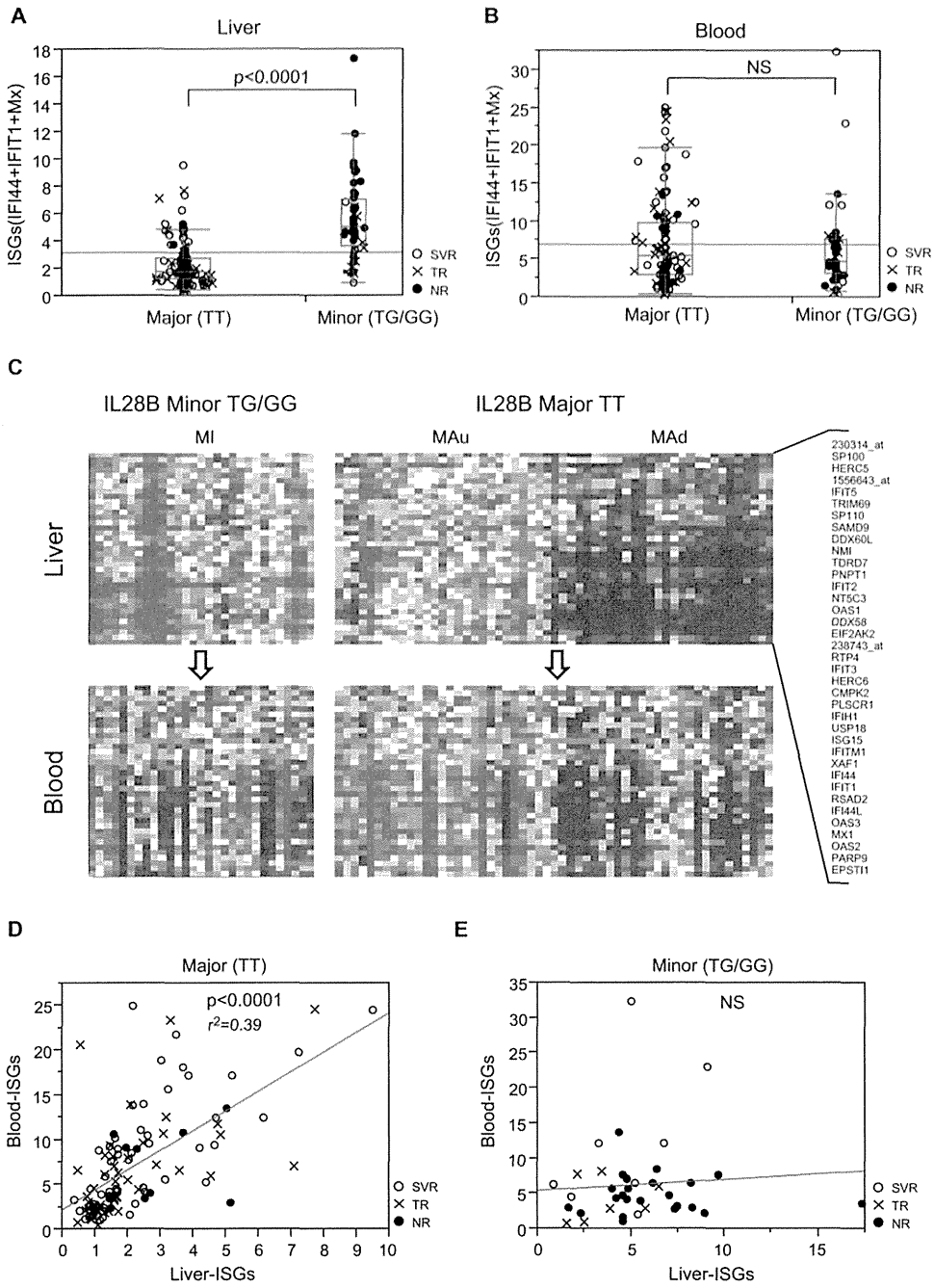

Fig. 1. Comparison of ISG expression in liver and blood of patients with different IL28B genotypes. (A and B) RTD-PCR results of mean ISG expression (IFI44-IFIT1+Mx1) in liver (A) and blood (B) of IL28B major (MAu/Mad) and minor (MI) genotype patients. (C) One-way hierarchical clustering analysis of 85 patients using 37 representative ISGs derived from liver (upper) and blood (lower). (D and E) Correlation of mean ISG expression (IFI44-IFIT1+Mx1) in liver and blood of IL28B major (MA; D) and minor (MI; E) genotype patients.

MI patients than in MAu and MAd patients (Supporting Fig. 4A,B). To support these findings, we examined the expression of 24 surface markers of immune cells in CLL, including dendritic cells (DCs), natural killer (NK) cells, macrophages, T cells, B cells, and granulocytes (Supporting Fig. 5A). The expression of immune cell-surface markers was repressed in MI patients, compared to MAu and MAd patients. Furthermore, whole-liver expression profiling in 85 patients showed the reduced expression of these surface markers in MI patients, compared to MAu and MAd patients (Supporting Fig. 5B). These results indicated that fewer immune cells had infiltrated the liver lobules of MI patients.

In addition to these findings, various chemokines, such as CC chemokine ligand (CCL)19, CCL21, CCL5, and chemokine (C-X-C motif) ligand (CXCL)13, which are important regulators for the recruitment of DCs, NK cells, T cells, and B cells in the liver, were significantly down-regulated in MI patients, compared to MAd and MAu patients (Supporting Fig. 4C-F).

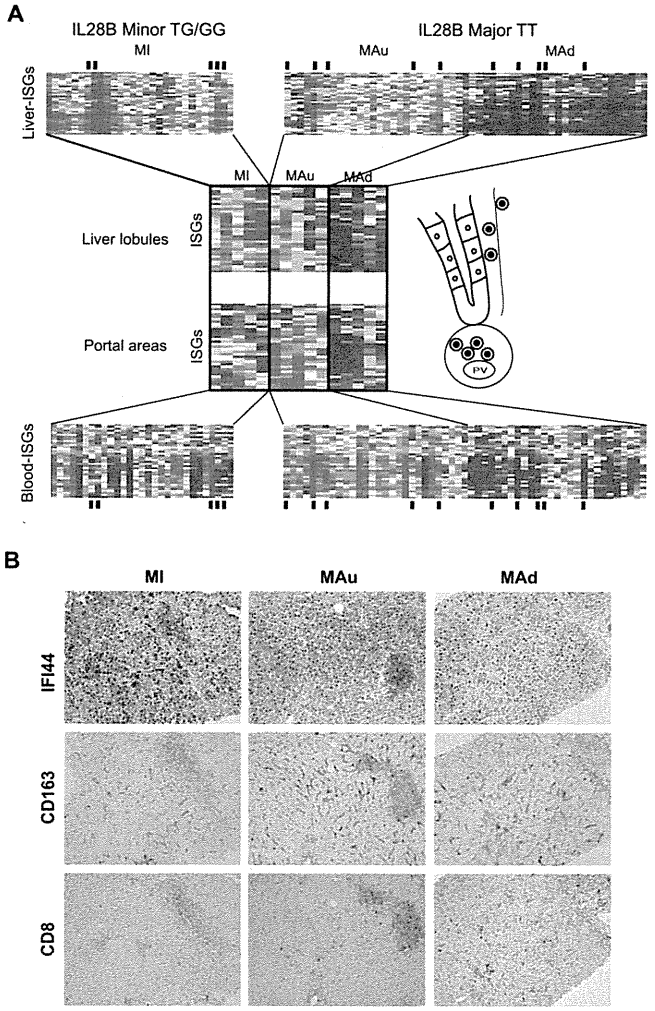

Fig. 2. LCM and IHC staining of biopsied liver specimens. (A) Comparison of the ISG expression pattern of whole liver (upper), CLLs (upper middle), CPAs (lower middle), and blood (bottom). CLLs and CPAs were obtained from 5 MI, MAu, and MAd patients, who are indicated by small black bars. (B) IHC staining of IFI44, CD163, and CD8 in MI, MAu, and MAd patients.

Hepatic ISG Expression Is Significantly Correlated With IL28A/B, but not IFN-α or IFN-β. The lower number of immune cells in the liver lobules of MI patients implies that reduced levels of IFN are produced from DCs, macrophages, and so on. These findings prompted us to examine the relationship between hepatic ISGs and IFN-α, IFN-β, IL29/IFN-λ1, and IL28A/B in CHC patients. Hepatic ISG expression was significantly correlated with IL28A/B, but not IFN-β (Fig. 3A-C) or IFN-α (data not shown) in MAu, MAd, and MI patients. Expression of IL29 was correlated with hepatic ISG expression only in MAu patients. These results indicate that hepatic ISGs would be mainly induced by IL28A/B in CHC patients. Interestingly, the correlation between hepatic ISGs and IL28A/B was strongest in MA patients ($P < 0.0001$ in MAu; $P = 0.0006$ in MAd), whereas rather a weak correlation was observed in MI patients ($P = 0.015$). Moreover, the ratio of hepatic ISGs to IL28A/B was larger in MI patients than in MA patients (S = 0.061 in MI; S = 0.028 in MAu; S = 0.020 in MAd), suggesting the presence of additional factors that can induce expression of ISGs in MI patients. Therefore, we evaluated the expression of the recently discovered IFN-λ4 in MI patients. Interestingly, there was a significant correlation between hepatic ISG and IFN-λ4 expression ($P = 0.0003$; Fig. 3C).

Wingless-Related MMTV Integration Site 5A and Its Receptor, Frizzled Receptor 5, Are Significantly Up-Regulated in the Liver of Patients With the IL28B MI. IFN-λ4 is a promising factor to induce ISG expression in MI patients,[8] and the functional relevance of IFN-λ4 for the pathogenesis of CHC is under investigation. We searched for other factors that could induce ISG expression in MI patients. A closer observation of gene expression profiling in CLLs obtained by LCM demonstrated that WNT signaling was specifically up-regulated in MI patients

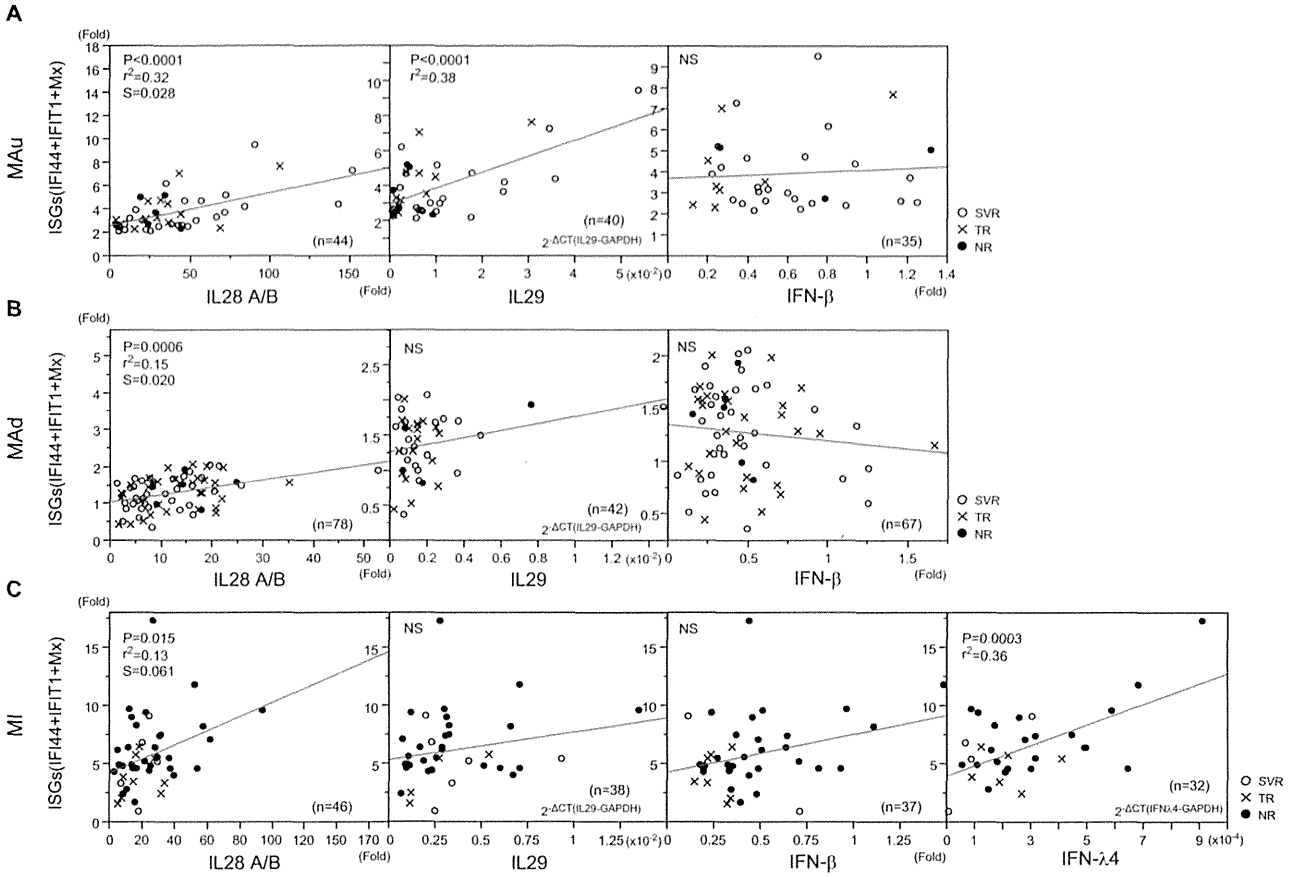

Fig. 3. Correlation analysis of hepatic ISGs and IL28A/B, IL29, IFN-β, and IFN-λ4. Correlation of mean ISG (IFI44+IFIT1+Mx1) and IL28A/B, IL29, IFN-β, and IFN-λ4 expression was evaluated in MAu (A), MAd (B), and MI (C) patients. [Color figure can be viewed in the online issue, which is available at wileyonlinelibrary.com.]

(Supporting Fig. 6). Further observation enabled us to identify that the WNT ligand, wingless-related MMTV integration site 5A (WNT5A), and its receptor, frizzled receptor 5 (FZD5), were up-regulated in MI patients. RTD-PCR results on 168 liver-biopsied samples confirmed the significant up-regulation of WNT5A and FZD5 in MI patients, compared to MAu and MAd patients (Fig. 4A,B). Interestingly, WNT5A expression was negatively correlated with chemokine expression (Supporting Fig. 7). IHC staining showed up-regulation of FZD5 in liver lobules of MI patients, but not in MAu or MAd patients (Fig. 4C). WNT5A expression was significantly correlated with hepatic ISG expression in MI and MAd patients (Fig. 4D). Interestingly, we found a weak, but significant, correlation between WNT5A and IFN-λ4 expression in MI patients (Fig. 4E).

WNT5A Induces ISG Expression, but Stimulates HCV Replication in Huh-7 Cells. To examine the functional relevance of up-regulated expression of WNT5A in MI patients, we first evaluated expression levels of WNT5A and ISGs (2′-5′-oligoadenylate synthetase 2 [OAS2], Mx1, IFI44, and IFIT1) in two immortalized human hepatocyte cell lines, THLE-5b and TTNT cells (Supporting Materials and Methods), and one human hepatoma cell line, Huh-7 cells (Supporting Fig. 8A,B). WNT5A was moderately expressed in THLE-5b and TTNT cells, whereas its expression in Huh-7 cells was minimal. Interestingly, ISG expression in these cells correlated well with expression of WNT5A (Supporting Fig. 8B). Small interfering RNA (siRNA) to WNT5A efficiently repressed WNT5A expression to ~20% of the control in THLE-5b cells, and in this condition, ISG expression was significantly decreased to 30%-50% of the control (Supporting Fig. 8C). Conversely, transduction of WNT5A using a lentivirus expression system in Huh-7 cells significantly increased OAS2 expression (Supporting Fig. 8D), as well as Mx1 and IFIT1 expression (data not shown), in the presence and absence of HCV infection. Surprisingly, HCV replication, as determined using Gaussia luciferase activity, increased in WNT5A-transduced cells (Supporting Fig. 8E). Furthermore, WNT5A-transduced cells supported more HCV replication than

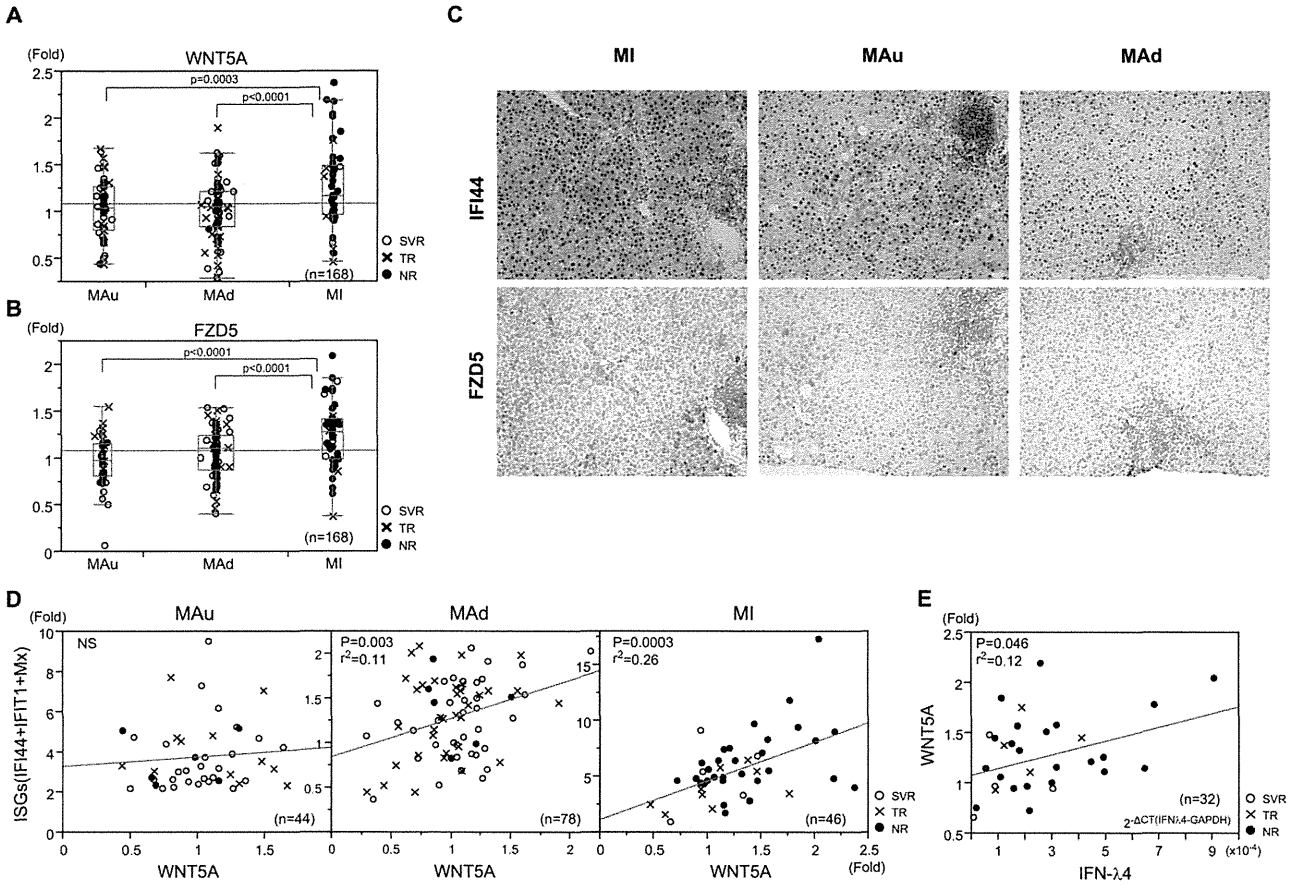

Fig. 4. WNT5A and FZD5 are up-regulated in IL28B MI patients. (A) RTD-PCR results of WNT5A expression in liver of MAu, MAd, and MI patients. (B) RTD-PCR results of FZD5 expression in liver of MAu, MAd, and MI patients. (C) IHC staining of IFI44 and FZD5 expression in liver of MAu, MAd, and MI patients. (D) Correlation of mean ISG (IFI44+IFIT1+Mx1) and WNT5A expression in liver of MAu, MAd, and MI patients. (E) Correlation of WNT5A and IFN-λ4 expression in liver of MI patients.

nontransduced cells under IFN treatment (Supporting Fig. 8F).

WNT5A-FZD5 Signaling Induces the Expression of the Stress Granule Protein, GTPase-Activating Protein (SH3 Domain)-Binding Protein 1, Which Supports HCV Replication. These findings were further confirmed by using Huh-7 cells that were continuously infected with Japanese fulminant hepatitis type 1 (JFH-1; Huh7-JFH1), which is a genotype 2a HCV isolate.[9] Interestingly, expression of WNT5A in Huh7-JFH1 cells was significantly up-regulated, compared with uninfected Huh-7 cells, and showed an equivalent expression level with THLE-5b cells (Fig. 5A). siRNA to WNT5A efficiently repressed WNT5A expression to ~20% of the control, and in this condition, ISG expression (IFI44 was not expressed in Huh-7 cells), HCV RNA, and infectivity were repressed to 25%-65%, 60%, and 40% of the control, respectively (Fig. 5B and Supporting Fig. 9A). Interestingly, CXCL13 expression was significantly increased in this condition. We evaluated the expression of GTPase-activating protein (SH3 domain)-binding protein 1 (G3BP1), a recently recognized stress granule (SG) protein that supports HCV infection and replication.[10] Expression of G3BP1 was repressed to 60% of the control by knocking down WNT5A. Conversely, overexpression of WNT5A in Huh7-JFH1 cells significantly decreased CXCL13 expression and increased HCV RNA, infectivity, and G3BP1 expression (Fig. 5C and Supporting Fig. 9B). A recent report demonstrated that G3BP1 is a disheveled (DVL)-associated protein that regulates WNT signaling downstream of the FZD receptor.[11] Knocking down FZD5 in Huh7-JFH1 cells significantly reduced the expression of DVL1-3, G3BP1, Mx1, and IFIT1 as well as HCV infectivity (Supporting Fig. 9C,D). Interestingly, G3BP1 expression was significantly up-regulated in liver of MI patients (Fig. 5D). Furthermore, G3BP1 expression was significantly correlated with WNT5A expression in liver of the CHC patients (Fig. 5E). More dramatically, a strong correlation was observed between expression of FZD5 and G3BP1 in liver of CHC patients (Fig. 5F).

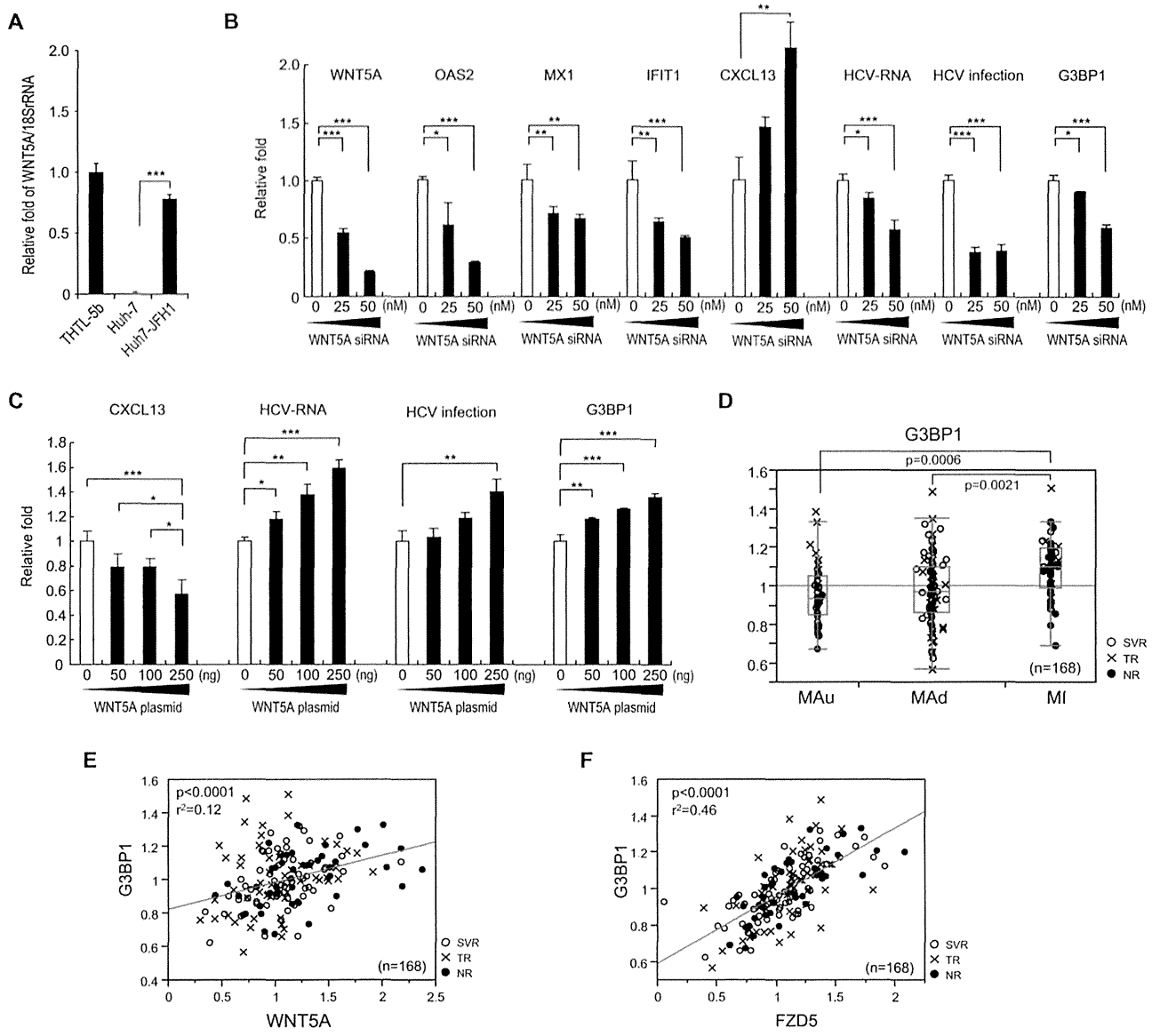

Fig. 5. Relationship between WNT5A and FZD5 signaling and the SG protein, G3BP1. (A) WNT5A expression in THLE-5b, Huh-7, and Huh7-JFH1 cells. (B) Knocking down WNT5A and changes of OAS2, Mx1, IFIT1, CXCL13, and G3BP1 expression, HCV RNA, and infectivity in Huh7-JFH1 cells. (C) Overexpression of WNT5A after transfection with pCMV-WNT5A and decrease in CXCL13 expression and increase in HCV RNA, infectivity, and G3BP1 expression. (A-C) Experiments were performed in duplicate and repeated three times (n = 6). Values are the means ± standard error. *$P < 0.05$; **$P < 0.01$; ***$P < 0.005$. (D) RTD-PCR results for G3BP1 expression in liver of MAu, MAd, and MI patients. (E) Correlation of WNT5A and G3BP1 expression in the liver. (F) Correlation of FZD5 and G3BP1 expression in the liver. [Color figure can be viewed in the online issue, which is available at wileyonlinelibrary.com.]

Discussion

The underlying mechanism for the association of the IL28B genotype with treatment responses to IFN-based therapy for HCV has not yet been clarified. We and others have shown that pretreatment up-regulation of hepatic ISGs was associated with an unfavorable treatment outcome[7,12,13] and was closely related to treatment-resistant MI IL28B, compared with treatment-sensitive MA IL28B.[6]

By comparing ISG expression in liver and blood, we found that their expression was correlated in MA patients, but not in MI patients. LCM analysis of ISG expression in CLLs and CPAs showed the loss of the correlation between CLLs and CPAs in MI patients (Fig. 2A). This might be the result of the impaired migration of immune cells into liver lobules that was demonstrated by decreased expression of immune cell-surface markers in CLLs by LCM (Supporting Fig. 5A) and IHC staining (Fig. 2B). Lymphocyte accumulation in the portal area (portal-tract-associated lymphoid tissue; PALT) might be involved in extravasation of lymphocytes from vessels in the portal area, but

others demonstrated that DCs appeared in the sinusoidal wall and passed through the space of Disse to PALT, where the draining lymphatic duct is located.[14] There should be an active movement of immune cells between liver lobules and PALT, as reflected by the correlation of ISG expression in CLLs and CPAs in the MA patients of this study.

ISGs were reportedly up-regulated in hepatocytes of treatment-resistant IL28B genotype patients, but were up-regulated in Kupffer cells of treatment-sensitive genotype patients.[15] Our results confirmed these findings; however, we also showed that expression of various immune cell-surface markers, such as those on DCs, NK cells, macrophages, T cells, B cells, and granulocytes, was lower in MI than in MA patients (Supporting Fig. 5). In addition, we showed that expression of various chemokines was also repressed in MI patients, compared to MA patients (Supporting Fig. 4C-F).

Up-regulation of pretreatment chemokine (C-X-C motif) ligand 10/interferon-gamma-induced protein 10 (CXCL10/IP-10) serum levels is also associated with an unfavorable treatment outcome.[16] CXCL10 expression in the liver was significantly correlated with hepatic ISG expression and was higher in nonresponders than in responders (Supporting Fig. 10). Our results support the usefulness of serum CXCL10 for prediction of treatment outcome. Chemokine (C-X-C motif) receptor 3 (CXCR3) expression, a receptor for CXCL10, was inversely correlated with hepatic ISG expression and was significantly lower in MI than in MA patients (Supporting Fig. 10).

The lower number of immune cells in the liver lobules of MI patients would imply the reduced production of IFN from DCs, macrophages, and so on. Correlation analysis showed that hepatic ISGs were mainly associated with type III IFNs (IL28A/B and IL29), but not type I IFNs (IFN-α or IFN-β), although a significant association with IL29 was only observed in MA patients with up-regulated ISGs. This might be related to the high serum ALT levels in MAu patients (Fig. 3). Closer examination of hepatic ISGs and IL28A/B suggested that factors other than IL28A/B might regulate ISG expression in MI patients. During the preparation of this study, IFN-λ4 was newly identified to be expressed in hepatocytes from treatment-resistant IL28B genotype patients.[8] Interestingly, we found a significant correlation between hepatic ISGs and IFN-λ4 in MI patients (Fig. 3C). Moreover, a closer examination of gene expression profiling in MI patients enabled us to detect up-regulation of the noncanonical WNT ligand, WNT5A. RTD-PCR analysis of 168 patients confirmed up-regulation of WNT5A and its receptor, FZD5, in MI patients. Importantly, WNT5A expression was significantly correlated with hepatic ISG expression in MI patients. A recent report showed that WNT5A induces expression of ISGs, increases sensitivity of keratinocytes to IFN-α,[17] and might be involved in the immune response to influenza virus infection.[18] Therefore, we examined the role of WNT5A in hepatocytes. Interestingly, expression of WNT5A and ISGs was well correlated, and knocking down WNT5A using siRNA reduced expression of ISGs in THLE-5b cells (Supporting Fig. 8). Conversely, transduction of Huh-7 cells with WNT5A using a lentivirus system increased expression of ISGs. Despite the increase in ISG expression, WNT5A did not suppress HCV replication, but rather increased it in Huh-7 cells (Supporting Fig. 8). These results were also confirmed by using Huh-7 cells continuously infected with JFH-1. By knocking down or overexpressing WNT5A in Huh7-JFH1 cells, we showed that HCV-RNA was positively regulated by WNT5A (Fig. 5B,C).

WNT5A and its receptor, FZD5, mediate noncanonical WNT signaling, such as planar cell polarity and the WNT-Ca^{2+}-signaling pathway through G proteins. WNT5A reportedly inhibits B- and T-cell development by counteracting canonical WNT signaling.[19] We found that G3BP1, an SG assembly factor, was up-regulated by WNT5A (Fig. 5C). SGs were reportedly formed by endoplasmic reticulum stress, followed by HCV infection, and localized around lipid droplets with HCV replication complexes.[10] G3BP1 contributes to SG formation and increases HCV replication and infection in Huh-7 cells.[10] Moreover, a recent report demonstrated that G3BP1 is a DVL-associated protein that regulates WNT signaling downstream of the FZD receptor.[11] In this study, repression of WNT5A or FZD5 significantly reduced expression of DVL1-3, G3BP1, Mx1, and IFIT1 as well as HCV infectivity in Huh7-JFH1 cells (Fig. 5 and Supporting Fig. 9).

Importantly, we found a significant correlation between WNT5A and G3BP1 expression in liver tissue samples (Fig. 5E). We also found a significant correlation between FZD5 and G3BP1 expression in liver tissue samples (Fig. 5F). Thus, up-regulated noncanonical WNT5A-FZD5 signaling participates in the induction of ISG expression, but preserves HCV replication and infection in hepatocytes by increasing levels of the SG protein, G3BP1. These findings may explain the pathophysiological state of the treatment-resistant phenotype in MI patients.

In this study, we demonstrated impaired immune cell infiltration of the liver in treatment-resistant IL28B genotype patients, and we also demonstrated

that up-regulation of hepatic ISGs in treatment-resistant IL28B genotype patients was mediated by multiple factors, including IL28A/B, IFN-λ4, and WNT5A. We found a significant negative correlation between WNT5A and various chemokines in liver of CHC patients (Supporting Fig. 7). Interestingly, WNT5A directly repressed one of these chemokines, CXCL13, a B-lymphocyte chemoattractant, in HCV-infected hepatocytes. These results indicate that loss of immune cells from the liver may be associated with the induction of other inflammatory factors, such as WNT5A, in MI patients, although we did not identify which cells express WNT5A. Further studies are needed to explore their functional relevance in the pathogenesis of CHC.

Acknowledgment: The authors thank Mina Nishiyama for her technical assistance.

References

1. Fried MW, Shiffman ML, Reddy KR, Smith C, Marinos G, Goncales FL, Jr., et al. Peginterferon alfa-2a plus ribavirin for chronic hepatitis C virus infection. N Engl J Med 2002;347:975-982.
2. Zeuzem S, Andreone P, Pol S, Lawitz E, Diago M, Roberts S, et al. Telaprevir for retreatment of HCV infection. N Engl J Med 2011;364:2417-2428.
3. Ge D, Fellay J, Thompson AJ, Simon JS, Shianna KV, Urban TJ, et al. Genetic variation in IL28B predicts hepatitis C treatment-induced viral clearance. Nature 2009;461:399-401.
4. Suppiah V, Moldovan M, Ahlenstiel G, Berg T, Weltman M, Abate ML, et al. IL28B is associated with response to chronic hepatitis C interferon-alpha and ribavirin therapy. Nat Genet 2009;41:1100-1104.
5. Tanaka Y, Nishida N, Sugiyama M, Kurosaki M, Matsuura K, Sakamoto N, et al. Genome-wide association of IL28B with response to pegylated interferon-alpha and ribavirin therapy for chronic hepatitis C. Nat Genet 2009;41:1105-1109.
6. Honda M, Sakai A, Yamashita T, Nakamoto Y, Mizukoshi E, Sakai Y, et al. Hepatic ISG expression is associated with genetic variation in interleukin 28B and the outcome of IFN therapy for chronic hepatitis C. Gastroenterology 2010;139:499-509.
7. Honda M, Nakamura M, Tateno M, Sakai A, Shimakami T, Shirasaki T, et al. Differential interferon signaling in liver lobule and portal area cells under treatment for chronic hepatitis C. J Hepatol 2010;53:817-826.
8. Prokunina-Olsson L, Muchmore B, Tang W, Pfeiffer RM, Park H, Dickensheets H, et al. A variant upstream of IFNL3 (IL28B) creating a new interferon gene IFNL4 is associated with impaired clearance of hepatitis C virus. Nat Genet 2013;45:164-171.
9. Wakita T, Pietschmann T, Kato T, Date T, Miyamoto M, Zhao Z, et al. Production of infectious hepatitis C virus in tissue culture from a cloned viral genome. Nat Med 2005;11:791-796.
10. Garaigorta U, Heim MH, Boyd B, Wieland S, Chisari FV. Hepatitis C virus (HCV) induces formation of stress granules whose proteins regulate HCV RNA replication and virus assembly and egress. J Virol 2012;86:11043-11056.
11. Bikkavilli RK, Malbon CC. Arginine methylation of G3BP1 in response to Wnt3a regulates beta-catenin mRNA. J Cell Sci 2011;124:2310-2320.
12. Sarasin-Filipowicz M, Oakeley EJ, Duong FH, Christen V, Terracciano L, Filipowicz W, Heim MH. Interferon signaling and treatment outcome in chronic hepatitis C. Proc Natl Acad Sci U S A 2008;105:7034-7039.
13. Chen L, Borozan I, Feld J, Sun J, Tannis LL, Coltescu C, et al. Hepatic gene expression discriminates responders and nonresponders in treatment of chronic hepatitis C viral infection. Gastroenterology 2005;128:1437-1444.
14. Kudo S, Matsuno K, Ezaki T, Ogawa M. A novel migration pathway for rat dendritic cells from the blood: hepatic sinusoids-lymph translocation. J Exp Med 1997;185:777-784.
15. Chen L, Borozan I, Sun J, Guindi M, Fischer S, Feld J, et al. Cell-type specific gene expression signature in liver underlies response to interferon therapy in chronic hepatitis C infection. Gastroenterology 2010;138:1123-1133.e1-3.
16. Askarieh G, Alsio A, Pugnale P, Negro F, Ferrari C, Neumann AU, et al. Systemic and intrahepatic interferon-gamma-inducible protein 10 kDa predicts the first-phase decline in hepatitis C virus RNA and overall viral response to therapy in chronic hepatitis C. HEPATOLOGY 2010;51:1523-1530.
17. Romanowska M, Evans A, Kellock D, Bray SE, McLean K, Donandt S, Foerster J. Wnt5a exhibits layer-specific expression in adult skin, is upregulated in psoriasis, and synergizes with type 1 interferon. PLoS One 2009;4:e5354.
18. Shapira SD, Gat-Viks I, Shum BO, Dricot A, de Grace MM, Wu L, et al. A physical and regulatory map of host-influenza interactions reveals pathways in H1N1 infection. Cell 2009;139:1255-1267.
19. Staal FJ, Luis TC, Tiemessen MM. WNT signalling in the immune system: WNT is spreading its wings. Nat Rev Immunol 2008;8:581-593.

OPEN

Gene Therapy (2015), 1–9
© 2015 Macmillan Publishers Limited All rights reserved 0969-7128/15
www.nature.com/gt

ORIGINAL ARTICLE

Preferable sites and orientations of transgene inserted in the adenovirus vector genome: The E3 site may be unfavorable for transgene position

M Suzuki, S Kondo, Z Pei[1], A Maekawa, I Saito and Y Kanegae

The adenovirus vector (AdV) can carry two transgenes in its genome, the therapeutic gene and a reporter gene, for example. The E3 insertion site has often been used for the expression of the second transgene. A transgene can be inserted at six different sites/orientations: E1, E3 and E4 sites, and right and left orientations. However, the best combination of the insertion sites and orientations as for the titers and the expression levels has not sufficiently been studied. We attempted to construct 18 AdVs producing GFP or LacZ gene driven by the EF1α promoter and Cre gene driven by the α-fetoprotein promoter. The AdV containing GFP gene at E3 in the rightward orientation (GFP-E3R) was not available. The LacZ-E3R AdV showed 20-fold lower titer and 50-fold lower level of fiber mRNA than the control E1L AdV. Notably, we found four aberrantly spliced mRNAs in the LacZ-E3L/R AdVs, probably explaining their very low titers. Although the transgene expression levels in the E4R AdVs were about threefold lower than those in the E1L AdVs, their titers are comparable with that of E1L AdVs. We concluded that E1L and E4R sites/orientations are preferable for expressing the main target gene and a second gene, respectively.

Gene Therapy advance online publication, 15 January 2015; doi:10.1038/gt.2014.124

INTRODUCTION

First-generation (E1 deleted) adenovirus vectors (FG AdVs), which lack the E1 and E3 regions, are popularly used in basic studies to elucidate gene functions, and have been employed for gene therapy.[1–4] Because the DNA fragments of up to about 7 kilobases (kb) in total can be inserted into the AdV genome, the AdVs are frequently used to produce two proteins simultaneously from two independent transgenes expressing both the target gene and the reporter gene, for example. In the studies using the cultured cells and in the animal experiments, the GFP and luciferase are used as the reporters. Recently, positron emission tomography has clinically been used in patients for diagnoses and in experimental animal models. Therefore, the AdVs containing both the therapeutic gene and the positron emission tomography reporter gene would be valuable in the gene therapy fields, because the therapeutic effects, the vector duration and distribution can simultaneously be monitored.[5–8] Probably one would wish for high-titer AdVs with the highest expression for the therapeutic gene and with the second highest for the reporter gene not causing any trouble, if the insertion sites and orientations in the AdV genome can be chosen. However, the titers and the expression levels of the AdVs may considerably be influenced by the sites and orientations of the transgenes. Such information may be very valuable for construction of the best vector, especially in the vector containing both the therapeutic gene and the reporter gene.

The simultaneous expression of two genes could be achieved by inserting the two genes into the E1 site under the control of a single prompter using the internal ribosomal entry sites or using porcine teschovirus-1 2A.[9,10] In the former approach, the expression of the second gene might be influenced by the sequences between internal ribosomal entry sites and its initiation codon, and in the latter, the manipulation is necessary to remove the stop codon of the first gene and to adjust the frames of the two genes. When two genes driven by the independent promoters are inserted into the E1 site, they might interfere with each other. However, when two independent expression units are inserted in different sites in the AdV genome, no interference occurs. Moreover, the advantage of this approach is that the main target gene can easily be changed using the AdV cassette that already contains the reporter gene.

There are three insertion sites and two orientations: a transgene can be inserted into the AdV genome by substitution of the E1 or E3 gene and by simple insertion at a position upstream of the E4 gene. Therefore, there are six different possible sites/orientations for any given transgene. Moreover, not only the potent promoters such as EF1α but also tissue-specific promoters such as α-fetoprotein (AFP) can also be employed. Although the studies examining which sites/orientations are superior to others are practically important, they have been very limited[11,12] and systematic analyses have not been reported so far.

As it is known that the expression level of a transgene varies considerably depending on the site in the cell chromosome of the human genome, the phenomenon is called the 'position effect'.[13,14] Although CG-methylation in the cell chromosome is clearly one reason, it is not observed in the AdV genome. Therefore, it would be of interest to examine whether the 'position effect' might also be observed similarly in the AdV genome for the potent promoter and for the tissue-specific promoter.

Laboratory of Molecular Genetics, The Institute of Medical Science, The University of Tokyo, Minato-ku, Tokyo, Japan. Correspondence: Dr Y Kanegae, Laboratory of Molecular Genetics, The Institute of Medical Science, The University of Tokyo, 4-6-1 Shirokanedai, Minato-ku, 108-8639, Tokyo, Japan.
E-mail: kanegae@ims.u-tokyo.ac.jp
[1]Current address: CDM (Contract Development & Manufacturing) center, Takara Bio Inc., 3-4-1 Seta, Otsu, Shiga, Japan.
Received 15 August 2014; revised 5 November 2014; accepted 20 November 2014

FG AdVs retain almost all viral genes. They are normally not expressed in the target cells, because E1A protein, the essential transactivator for expression of all other viral genes, is not present. However, there is one report of splicing of aberrant mRNAs from the inserted foreign genes to a viral gene.[15] In this case, the aberrant mRNAs are transcribed by strong foreign promoters and produce transgene-viral gene fusion proteins, which elicit strong immune responses. However, it is not known whether the production of the aberrant gene product between the inserted transgene and viral gene is rare or not.

In this study, we examined the AdV titers and expression levels of an identical transgene inserted at the E1, E3 and E4 sites. We used three transgenes, namely, GFP, LacZ and Cre, and two promoters, namely, the potent EF1α promoter and the cancer-specific AFP promoter, and attempted to construct AdVs using all combinations, that is, 18 AdVs, and succeeded in constructing 17 of them. We found that insertion at the E1 and E4 sites yielded mostly high titers, whereas the one at the E3 yielded variable titers. Surprisingly, four aberrantly spliced mRNAs between the transgenes and viral genes were found in the vector obtained by insertion at the E3 site, which was probably the reason for the very low titers. As for the expression levels, clear differences were observed among the vectors obtained with insertion at the E1, E3 and E4 sites despite using the identical transgene, indicating that the position effect was certainly present for the AdV genome and that aberrant splicing may, at least in part, explain this effect. We also propose a strategy to avoid generation of the aberrantly spliced mRNAs.

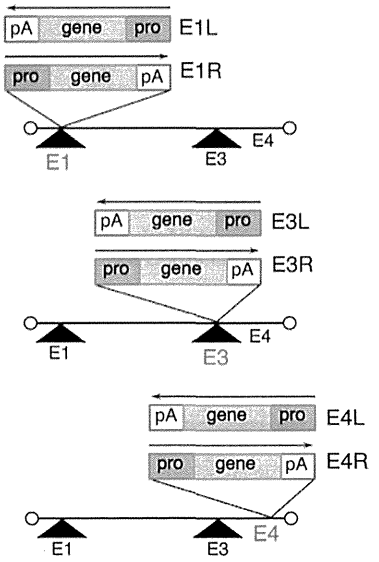

Figure 1. The FG AdV structures of six different site/orientations in all possible combinations. The box containing 'pro,' 'gene' and 'pA' represents the expression unit and the arrows show the orientation of transcription. 'pro,' EF1α and AFP promoter; gene, GFP, LacZ and Cre; pA, rabbit β-globin polyadenylation signal. For example, the vector containing the transgene at the E1 insertion site and in the left orientation is denoted as 'E1L.'

RESULTS

The vector titers were significantly influenced by the insertion sites and orientations of the transgene

We first examined whether the vector titers were influenced by the site/orientations of the transgenes containing a potent EF1α promoter. Towards this end, we attempted to construct six GFP-expressing (EF-GFP) and six LacZ-expressing (EF-LacZ) vectors in all possible combinations, that is, the E1, E3 and E4 insertion sites and the two orientations (Figure 1), and measured the vector titers (Figure 2a) (hereinafter, the vectors will be designated as per the following; the vectors containing the GFP gene and LacZ gene at the E1 insertion site and in the left orientation shall be denoted as G-E1L and Z-E1L vectors, respectively). Among the GFP-expressing vectors, high titers were obtained for G-E1L, G-E3L, G-E4L and G-E4R vectors (Figure 2a, bars 1, 3, 5 and 6), while the titer for the G-E1R vector was lower (bar 2). Notably, the G-E3R vector, that is, vector with the GFP transgene inserted in the E3 site in the rightward orientation, could not be obtained despite three independent attempts (bar 4, denote '×'). Therefore, although exactly the same EF1α-GFP expression unit was inserted in these vectors, the sites and orientations exerted considerable influence on the vector titers and even determined whether the vector was available or not. Similar results were obtained for vectors expressing LacZ: the titers of the Z-E1L, Z-E4L and Z-E4R vectors (bars 7, 11 and 12) were high, and that of the Z-E1R vector was also low (bar 8). However, the results of insertion at the E3 site differed for GFP and LacZ. The titer ratio of Z-E3L was significantly lower than that of G-E3L (compare bars 3 and 9, described later), and the Z-E3R vector was available, although its titer was extremely low (bar 10). Therefore, the GFP gene and LacZ gene themselves influenced the vector titers.

Then, we constructed six vectors containing the AFP promoter and Cre gene (AFP-Cre) and measured their titers (Figure 2b). Although these vectors contained the AFP promoter and Cre gene, this transgene unit served as a nonfunctional DNA, because the AFP promoter, which is hepatocarcinoma-cell-specific, is not active in the 293 cells. The titers of the all six vectors were very similar (Figure 2b). Thus, the site/orientation does not always influence the vector titers, and it appeared that there may be some specific reasons why the titers were low for vectors containing the EF1α promoter expressing the GFP and LacZ genes.

Aberrant chimera mRNAs were produced in the vectors containing the expression unit at the E3 site

The E3 transgene is present within the large intron from the major late promoter (MLP) to the fiber gene (Figure 3a, except the first). We previously reported an aberrant splicing from a cryptic donor site present in the LacZ gene to the viral pIX acceptor site, which produces a LacZ-pIX fusion protein.[15] Therefore, we speculated that similar aberrant splicing might occur for the LacZ gene inserted at the E3 site.

Total RNA was prepared from the 293 cells infected with the E3R vector and reverse-transcribed to detect such aberrantly spliced mRNA spanning from the LacZ cryptic donor site to the possible fiber acceptor site, which is the only acceptor site present downstream of the LacZ donor site. In fact, we identified an aberrant mRNA spliced from this LacZ donor to the fiber acceptor (Figure 3a, second; Figure 3b, 0.7-kb band). The splicing donor site in the LacZ gene was identical to that of the reported LacZ gene inserted at E1 site to the viral pIX acceptor site, and the fiber acceptor site was the same as that normally spliced from the MLP donor site (Supplementary Table S1). This is quite abnormal because, in general, splicing occurs between only specific donor and acceptor sites, suggesting that an inserted transgene could disturb normal splicing.

We also examined whether any other aberrantly spliced mRNA upstream of the transgene was present or not. Surprisingly, we also detected an abnormal mRNA spliced from the donor site of the third exon of the viral MLP to the acceptor site of the second exon of the EF1α promoter (Figure 3a, third; Figure 3b, 1.2-kb band; the junction sequence is shown in Supplementary Table S1). These results mean that the normal splicing from the MLP donor to the fiber acceptor are doubly competed with aberrant splicing

© 2015 Macmillan Publishers Limited